8

Charged Particle Irradiation Studies on Bismuth Based High Temperature Superconductors & MgB_2; A Comparative Survey

S.K.Bandyopadhyay
Variable Energy Cyclotron Centre, 1/AF, Bidhan Nagar, Kolkata-700 064 India

1. Introduction

In the field of superconductivity, the discovery of Lanthanum Cuprate ($La_{2-x}Sr_xCuO_4$) ushered in a new era- the so called High Tc superconductors (HTSC). High Tc Cuprate Superconductors are quite intriguing and unique in their behaviour in contrast to their low Tc counterparts. Defects and disorder play a crucial role in controlling various physical properties like Tc, resistivity, Critical Current Density (Jc) etc. in these hole doped superconductors. The nonstoichiometries in these compounds, in particular, with respect to oxygen bring out fascinating properties, oxygen playing the role of hole carrier. These compounds are based on layered perovskite structure. Superconductivity essentially resides in CuO_2 plane, with other layers containing multivalent metal ions functioning as charge reservoir layers, pumping holes or, electrons to the superconducting CuO_2 layer and thereby controlling the Cu-O-Cu coupling and Tc. The cuprates are essentially quasi 2-dimensional systems with a weak interlayer coupling along c-direction between two CuO_2 layers residing in ab-plane. This also gives rise to anisotropy in various physical properties like conductivity, Jc etc. It is seen that Tc increases in general with more number of CuO_2 layers and with more anisotropy. This millennium saw a non cuprate system MgB_2 which is quite simple compared to cuprates, yet with a fairly high Tc of 40K. This has got some similarity with the conventional superconductors in that it is BCS type superconductor with holes in the antibonding band of Boron, coupling with phonons of E_{2g} vibrational mode. MgB_2 possesses hexagonal AlB_2 type structure with Mg ions sandwitched between boron hexagons. Boron is sp^2 hybridised with in plane σ-band primarily participating in superconductivity and the out of plane π-band taking the role of conductivity like graphite, though it is a two band superconductor. Intra and interband scattering play a great role in controlling the superconducting and transport properties.

Charged particle irradiation introduces various kinds of point defects, line defects, etc. which have wide manifestations. In case of HTSC, irradiation produces drastic change in Tc and resistivity. We had observed an increase in Tc in $Bi_2Sr_2CaCuO_2$ (Bi-2212) by α and proton irradiation, which could be explained by irradiation induced knock out of oxygen in overdoped system [1-3]. With this end in view, we carried out irradiations of textured polycrystalline Bi-2212 and $(Bi,Pb)_2Sr_2Ca_2Cu_3O_{10+x}$((Bi,Pb)-2223) with 40MeV α and 15MeV protons at various does. We have also irradiated MgB_2 with Neon ions of 160 MeV available

at Variable Energy Cyclotron Centre, Kolkata. Energies of particles were selected considering the optimisation of nuclear reaction of the projectile with the sample and the range of particles in the sample. In case of HTSC Bi-cuprates, the purpose was to investigate the knock-out of oxygen caused by particle irradiation and its effects on superconductivity. For MgB_2, heavy ion like Neon was chosen to have effective damage as it was seen to be fairly insensitive to particle irradiation. In this article, we are highlighting the salient features of charged particle irradiation effects on HTSC and MgB_2 and analysing the remarkable differences.

The presentation is divided into following sections. The section 2 briefly describes irradiation effects on solids and in particular, the superconductors. In section 3, we describe the effects on Tc and resistivity of Bi-2212 and Bi-2223 and their qualitative difference due to light charged particle (proton and alpha particles) irradiation in the light of oxygen knock-out. Manifestation of this difference with respect to irradiation induced oxygen knock-out is in the nature and size of irradiation induced defects and their pinning potentials which control the enhancement of Jc due to irradiation. These aspects are discussed in section 4 with respect to proton irradiation on these systems. In section 5, we have dealt with heavy ion irradiation studies on MgB_2 and have brought out comparative studies.

2. Irradiation effects on solids

High energy charged particles interact with solids through two main processes-elastic and inelastic. Elastic collisions with solid target nuclei cause nuclear energy loss leading to displacement of atoms. Inelastic or electronic energy loss causes ionisation and excitation of atoms. The dissipation energy (-dE) of the incident particle of energy E for the distance (dx) traversed in solid target is expressed as:

$$(-dE/dx)_{total} = (-dE/dx)_{nuclear} + (-dE/dx)_{electronic} \quad (1)$$

The cross-sections of two processes depend on the energy and nature of the incident particle. Thus, for protons of energy 1MeV, electronic energy loss is ~$2x10^4$ times the nuclear energy loss, whereas for Argon ions of same energy, both are of comparable magnitude [4]. For low energy or, medium energy projectile, it is the displacement of atoms caused by nonionising energy loss (NIEL) through elastic collisions that are of most concern in condensed matter physics. If S_n is the energy deposited due to elastic collisions and E_d is the displacement energy of the target atom, then the number of displaced atoms is $S_n/2E_d$ [5]. If N is the total no. of atoms, the number of displacements that each atom suffers is $(S_n/2E_d)/N$. This is called the displacement per atom (d.p.a.) and is a measure of the nonionising energy deposited. For a particular irradiation, d.p.a. is proportional to the fluence or dose of irradiation. Moreover, it depends on the energy and the nature of the projectile as well as the atomic number of the target material. Thus, for same energy, heavy ions will have larger d.p.a. compared to light atoms. For a typical dose of $1x10^{15}$ particles/cm^2, d.p.a. for 40 MeV α-particles and 15 MeV protons in BSCCO are $1.26x10^{-4}$ and ~$1.2x10^{-5}$ respectively. D.P.A. is a measure of defect concentration.

In electronic energy loss, target atoms get ionised or, excited. During the deexcitation, heat is generated due to transfer of energy to vibrational modes of target atoms. This gives rise to amorphisation due to local heating effects. In case of high energy heavy ions, there is extensive amorphisation along the track of the projectile, giving rise to so called columnar defects. These are much effective as pinning centres in case of superconductors, particularly HTSC.

In the interaction of projectile particle with target atoms, we are concerned with the fates of the scattered projectile particle and the recoil atoms after collision. The projectile loses energy by collisions with the target atoms. Similarly, the target atoms with high recoil energy collide with other target atoms and in turn lose energy.
It is obvious that estimation of the total damage created by a single projectile necessitates following every collision that a projectile undergoes until it almost stops. Hence comes the need of some simulation program. The Monte Carlo method as applied in simulation techniques is more advantageous than the analytical formulations based on transport theory. The most commonly used simulation program is the one developed by Biersack et al [6] called TRIM (TRansport of Ions in Matter). In this program, the nuclear and electronic energy losses are assumed to be independent of each other. Particles lose energy in discrete amounts in nuclear collisions and continuously in electronic interactions.

2.1 Effects of irradiation induced defects on superconductors:

In case of superconductors, nonionising energy loss (NIEL) causing displacement of atoms plays a significant role in controlling physical properties like critical temperature, resistivity, critical current density etc. In conventional superconductors, point defects generated by radiation induced atomic displacements change electronic density of states around Fermi surface, causing thereby depression of Tc [7,8]. In case of high Tc superconductors also, it has been seen that atomic displacements caused by NIEL of incident particle control the change of Tc as a function of fluence [9,10]. NIEL causes anionic (oxygen) and cationic displacements and both play important roles in the change of Tc and resistivity by varying the carrier concentration. As discussed earlier, these superconductors are non-stoichiometric with respect to oxygen which controls the hole concentration in conducting CuO_2 planes. Thus, irradiation induced change in oxygen content is expected to bring forth change in carrier concentration resulting in changes in Tc and resistivity. Moreover, the irradiation induced knock-out would cause oxygen vacancies which can act as effective pinning centres, thereby causing enhancement of Jc. This makes the study of irradiation induced knock-out of oxygen so fascinating.
In YBCO system, particle irradiation generally causes knock-out of oxygen from Cu-O-Cu chain and leads to orthorhombic to tetragonal phase transition with oxygen deficiency. At high dose, metallic to semiconducting phase transition occurs [11]. These oxygen vacancy defects act as flux pinning centres. Activation energy for flux creep decreases with oxygen deficiency [12].

3. Charged particle irradiation effects on HTSC:

X-ray Diffraction patterns of some α-irradiated Bi-2212 and Bi-2223 samples along with the unirradiated ones are presented in Figs. 1 and 2 respectively. The characteristic reflection lines of the unirradiated samples are present in the irradiated samples. There have been slight shifts of 00l peaks in α-irradiated Bi-2212 samples towards lower angles compared to those of the unirradiated sample. There is an increase in c-parameter in the irradiated Bi-2212 samples. Normally, the holes or, oxygen causes an increase in positive character of the copper in CuO_2 plane. Thereby attraction of copper to apical oxygen atoms increases and decrease in c-parameter occurs. Also, Cu-O bond length decreases causing a decrease in a-parameter. In case of Bi-2212 irradiated with 40 MeV α, the increase in c-parameter can be

explained by the irradiation induced knock-out of oxygen. Thereby the hole carrier concentration in CuO_2 plane decreases, causing increases in both a and c-parameters. On the other hand, in case of Bi-2223, there has not been any change in c-parameter.

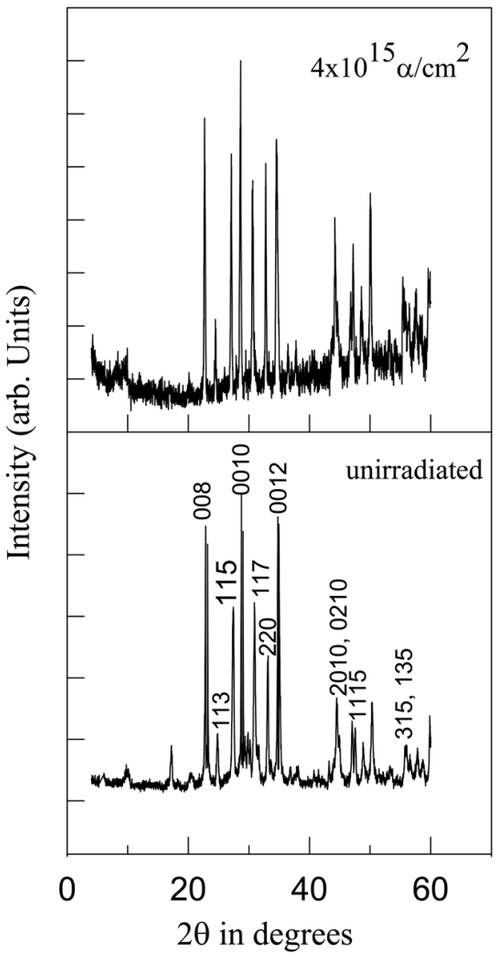

Fig. 1. XRD pattern of unirradiated and $4x10^{15}$ α/cm² polycrystalline of Bi-2212.

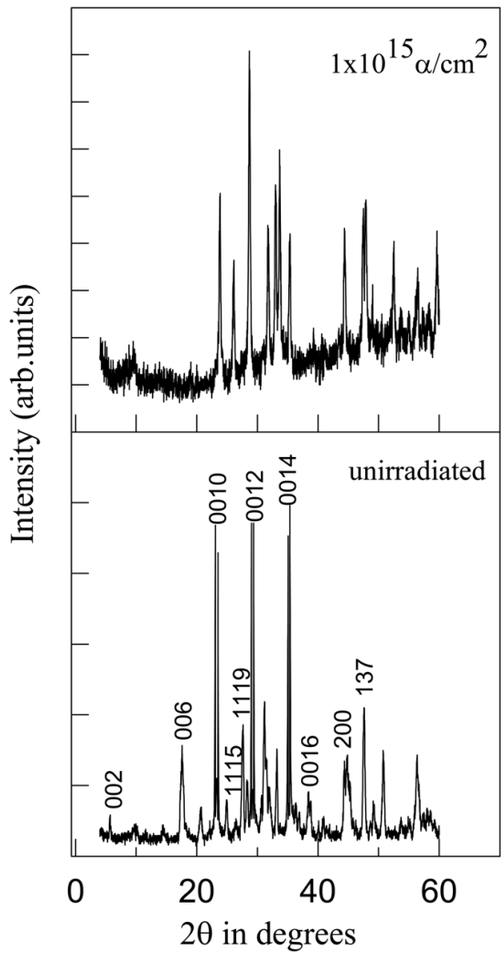

Fig. 2. XRD pattern of unirradiated and $1x10^{15}$ α/cm² polycrystalline of Bi-2223.

Resistivity versus temperature plots of some irradiated samples of 40MeV α-irradiated Bi-2212 polycrystal as compared to the unirradiated samples are presented in Figures. 3(a and b). Table-I shows the values of Tc(R=0), Tc(onset) and excess oxygen (determined by iodometry) as a function of fluence.

In case of Bi-2212 polycrystalline samples, oxygen contents have decreased with dose. The unrradiated polycrystalline Bi-2212 of Tc=73K has x value (i.e. oxygen content in excess to that of stoichiometry) of 0.204 as evident from iodometric estimations. Excess oxygen is the source of the hole carrier in these cuprates. Tc is related to the hole carrier density and hence excess oxygen content(x). In Bi-2212, Tc increases initially with x, goes to a maximum and then decreases with the increase of x following a typical dome shaped curve [13]. The excess oxygen contents corresponding to the peak values of Tc vary from 0.15 to 0.16 [13,14]. The excess oxygen in unirradiated polycrystalline Bi-2212 (0.204) corresponded to the right or the overdoped side of the Tc versus oxygen dome-shaped

curve [13]. As oxygen content of the unirradiated sample was in excess to that (~0.16) corresponding to the maximum Tc, it is expected that there would be an increase in Tc on reduction of oxygen content. Thus, the increase in Tc for the irradiated samples was due to the loss of excess oxygen. The peak of Tc(R=0) corresponds to a dose of ~$6x10^{15}\alpha/cm^2$ and the equivalent oxygen content is 0.10.

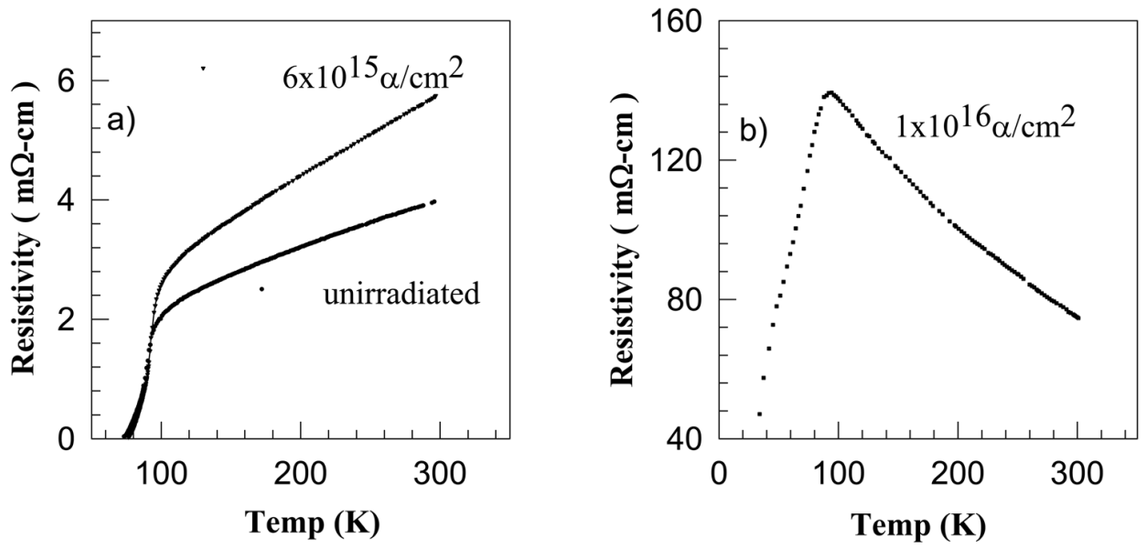

Fig. 3. (a) Resistivity of unirradiated, $6x10^{15}$ α/cm^2 and (b) highest dose ($1x10^{16}$ α/cm^2) of polycrystalline of Bi-2212 as a function of tempareture.

Dose (α/cm^2)	Tc(R=0) (K)	Tc(Onset) (K)	Excess Oxygen (x)
Bi-2212:			
0	73.1	90.5	0.204
$2x10^{15}$	74.3	92.3	0.190
$4x10^{15}$	75.8	94.8	0.150
$6x10^{15}$	76.3	92.7	0.100
$1x10^{16}$	<10.0	-	0.055
Bi-2223:			
0	112.0	122.0	0.100
$1x10^{15}$	111.0	122.0	0.100
$2x10^{15}$	108.0	122.0	0.100
$3x10^{15}$	105.8	121.8	0.100
$4x10^{15}$	103.6	121.6	0.096
$1x10^{16}$	64.0	94.0	0.096

Table I. Variation of Tc, Excess Oxygen and other parameters with dose for polycrystalline Bi-2212 and Bi-2223 irradiated with 40MeV α-particles.

Tc(onset) is the temperature at which grains become superconducting. The granular Tc is controlled by the lattice oxygen content. Hence, Tc(onset) is affected by x, the excess oxygen, whereas Tc(R=0) is controlled by the intergranular links too. In polycrystalline samples, grain boundaries are regions of the highest energy and most vulnerable for radiation damage like enhanced formation of defects, outdiffusion of oxygen etc., which lead to destruction of weak intergranular links and depression of Tc(R=0) even at lower doses of irradiation, whereas the granular Tc i.e. Tc(onset) is not affected.

It is the radiation induced destruction of weak intergranular links in polycrystalline samples that causes an increase in the transition width and fast decrease in Tc(R=0) of 40Mev α-irradiated Bi-2212 sample at higher dose where it is underdoped with respect to oxygen. This is reflected in the overdoped region too. In the overdoped region, irradiation induced knock-out of oxygen increases Tc on one hand and the destruction of intergranular links causes a decrease in Tc. Hence, Tc(R=0) versus excess oxygen curve is less sharp than that of Allgeier et al. [13], i.e. the increase of Tc (R=0) with dose is less compared to Tc (onset) in the overdoped region. It is because of this intergranular effects that the peak of Tc (R=0) corresponds to oxygen content of 0.10 and not 0.15 where the peaking of Tc(onset) occurs.

Unlike polycrystalline Bi-2212, there has been no increase in Tc(onset) and no change in oxygen content in particle irradiated Bi-2223. The irradiation induced knock-out of oxygen is absent in Bi-2223. In most cases (both proton and α-irradiation on Bi-2212 and Bi-2223), there are increases of transition widths (ΔTc).

The resistivity changed from metallic to insulating behavior by α-irradiation at a dose of $1x10^{16}\alpha/cm^2$ and higher for both Bi-2212 and Bi-2223. The nonlinear behavior of resistivity is indicative of localization of charge carriers caused by irradiation induced disorder. We analysed the non linear behavior of resistivity in the framework of variable range hopping (VRH). Normally, the resistivity in the insulating region is given by

$$\rho = \rho_0 \exp [(T_0 / T)^{1/(d+1)}] \quad (2)$$

where the hopping conduction of carriers occurs in d-dimension. Here, T_0 and ρ_0 are constants.

Thus, for 2-dimensional VRH, $\rho = \rho_0 \exp [(T_0 / T)^{1/3}$,

and for 3-dimensional VRH, $\rho = \rho_0 \exp [(T / T)^{1/4}]$.

In our case, the best fit was obtained in the case of Ln(ρ) vs. $(T)^{-1/4}$ plot in the temperature range of 256K to 115K for Bi-2212 and 190K to 120K for Bi-2223. Thus, the conduction in the non-metallic region proceeds through 3-Dimensional VRH. Similar metal to insulator transition was observed in $Bi_2Sr_2Ca_{1-x}Y_xCu_2O_{8+x}$ at x>0.5 [15,16]. Substituting Y(III) in Ca(II) site causes a lowering of carrier concentration. From the general phase diagram for these systems, it is now evident that, they are Mott-Hubbard insulators at very low carrier concentration and become superconducting as the carrier concentration is increased to a certain extent and the normal state behavior changes from insulator to metallic [17-20]. For the carrier concentration corresponding to the cross-over region from metal to insulator, the conduction is generally seen to occur through 3D-VRH [21].

The reasons for transition from metal to insulator behavior of the irradiated sample at the highest dose may be two fold: 1) lowering of carrier concentration due to the knock-out of oxygen, 2) generation of localisation caused by irradiation induced disorder [22]. There is a difference between the irradiation induced localizations in Bi-2212 and Bi-2223. In α-

irradiated Bi-2223, the change of carrier concentration due to change in oxygen content is not significant which is dominant in α-irradiated Bi-2212 as evident from iodometry. Rather localisation caused by the radiation induced disorder plays a major part in case of Bi-2223.

We have estimated the localisation length denoted as α^{-1}. For 3D VRH, α^{-1} is derived from T_0 using the following expression:

$T_0 = (16\alpha^3)/[k_B N(E_F)]$; $N(E_F)$ is the density of states at Fermi level and k_B is Boltzmann constant. For Bi-2212, the values of $N(E_F)$ obtained from specific heat data range from 1.25-5.62x10^{-2} states/eV/$Å^3$ (for three dimensions) [23,24]. We have taken the value ~1.8x10^{-2}states/eV/$Å^3$ [20]. The localisation length (α^{-1}) comes ~10.7Å. This value of α^{-1} is quite low compared to that (60-80Å) in the case of $Bi_2Sr_2Ca_{1-x}Y_xCu_2O_{10+x}$ in 3D-VRH regime at the cross-over of metal to insulator transition (for x=0.55) [21]. Our value is comparable to that for x=0.6. In case of Bi-2223, the localisation length (α^{-1}) comes 10.6Å, around five times the Cu-O bond length in CuO_2 plane.

The Cu-O bond in CuO_2 sheet is the strongest bond and it controls the lattice constants [25]. The other layers in the crystal structure are constrained to match the CuO_2 sheet and thus internal stress is generated within the crystal structure. The lattice stability in these cuprates is governed by a tolerance factor defined as:[26]

$$t=(A\text{-}O)/[2^{1/2}(B\text{-}O)]$$

In Bi-2212, A-O and B-O are bond lengths of Bi-O in rock salt block and Cu-O in perovskite block respectively. In perovskites, for stable structure, value of 't' should be as 0.8 <t <0.9 [36]. If the bond lengths are taken to be the sum of the ionic radii of the respective ions, then with $r_{(Bi^{3+})}$ =0.93 Å, $r_{(O^{2-})}$ =1.4 Å, $r_{(Cu^{2+})}$ =0.72 Å , 't' comes out to be 0.78 in Bi-2212, and is less than the value needed for structural stability and an internal strain is developed. Since the Cu-O bond is rigid, the strain due to lattice mismatch can be relieved by the increase of A-O bond length which can be attained either by substitution of Bi^{3+} by larger ion or by accommodating excess oxygen in the Bi-O layer. In undoped Bi-2212, the latter process occurs, whereby the Bi-O bond distance increases to 2.6 Å and the tolerance factor comes within proper range. This excess oxygen resides in Bi-O layer because of the repulsion of the lone pair of electrons in Bi^{3+}ion and oxygen along c-axis. The extra oxygen atoms form rows along a-axis and cause incommensurate modulation along b-axis [27]. They are not valence bound. The binding energy of these extra oxygen atoms is very low and hence they are vulnerable to be knocked out by energetic α-particles and protons depending on the amount of energy deposited by the projectile.

The decrease in oxygen content (or the knock-out of oxygen) caused by irradiation with charged particles from Bi-2212 sample can be understood to occur through following steps: 1) Appreciable oxygen vacancies are created by charged particle irradiation induced displacement at a dose > 1x10^{15} particles/cm^2; 2) These displaced oxygen atoms occupy pores which are energetically favourable to them; 3) These 'free' or labile oxygen molecules diffuse from pores to outside (of the sample) which is in vacuum (~10^{-6}torr) during irradiation [28]. This is the driving force for migration. The rate of oxygen atoms/molecules diffusing out is proportional to the atoms/molecules of oxygen present in pores. At room temperature, there is no reabsorption of oxygen by Bi-2212 as oxygen absorption needs activation energy and hence a net decrease in oxygen content occurs.

In Bi-2223 synthesised by partially doping Pb in Bi-site, the tensile stress in Bi-O layer is relieved by substitution of larger Pb^{2+} ion (1.2Å) in Bi^{3+} (0.93Å) site. So, Pb doped Bi-2223

does not accommodate excess oxygen significantly. Pb(II) substituting Bi(III) provides holes to CuO layer, thereby relieving its compressive stress. Hence there is no loosely bound oxygen to be knocked out. In Bi-2223, because of absence of loosely bound oxygen, only strong lattice bound oxygen comes into picture for being knocked out. TRIM-95 calculations show the number of oxygen atoms displaced by 40 MeV α-particles is ~5/ion in case of Bi-2223, whereas the same in case of Bi-2212 containing loosely bound oxygen is around 110/ion [28]. This gives rise to the difference in Bi-2212 and Bi-2223 with respect to oxygen knock-out. Manifestation of this difference was reflected in their behaviour in Tc and resistivity and also in Jc and pinning potential, as the irradiation induced knocked out oxygen vacancies play the role of flux pinning centres. Thus, Bi-2212 and Bi-2223 behave differently with respect to the enhancement of Jc and pinning potential, as will be revealed in the following section 4.

3. Jc and pinning potentials for irradiated BSCCO superconductors

The most important aspects of defects governing the physical properties of superconductors, in particular Jc and pinning, are their size and concentration. Pinning is intimately related to the size of defects and is maximum when the size of the defects is nearly same as vortex core. Hence to assay the pinning due to defects, it is essential to have an idea of concentration and size of defects. We are highlighting studies of defects and their pinning in proton irradiated BSCCO (Bi-2212 and Bi-2223) superconductors

Positron Annihilation Lifetime (PAL) study is a probe for assaying defect size and concentration. Positron annihilates with electrons of atoms. Absence of atoms or, vacancies causes trapping of positrons and hence enhancement of lifetime. More the size of vacancies, the more will be the lifetime of positrons. Moreover, there is some broadening of the annihilated γ spectra due to the angular momentum of the electrons with which the positron annihilation takes place. Thus, Doppler Broadened Positron Annihilation Radiation technique (DBPARL) also highlights about defects.

The positron lifetime spectra of Bi-2212 and Bi-2223 revealed three lifetimes – the longest one designated as τ_3 of 1.6-2.0 ns being the pick-off annihilation lifetime of ortho-positronium atoms, formed at the intergranular space. Among other life times, the shorter one τ_1 represents the combined effects of positrons annihilating in the bulk and those with free Bloch state residence time. Longer one τ_2 is the result of trapping of positrons in vacancy type defects with which we are mostly concerned regarding the size of defects. For unirradiated Bi-2212 and Bi-2223, the values of τ_2 are 284 and 274 ps respectively. These values indicate that the unirradiated Bi-2212 and Bi-2223 consist of defects essentially in form of divacancy and monovacancy respectively [29]. τ_2 increases for Bi-2212 up to the dose of $5x10^{15}$ proton/cm^2 and then decreases (Fig. 11). But, in case of Bi-2223, there is no significant change in τ_2 up to this dose compared to the unirradiated sample. From Table-II, we see that there is no significant change in the concentration of defects in Bi-2223, which is higher than Bi-2212 in unirradiated stage.

Increase in τ_2 and defect size of Bi-2212 are manifestations of irradiation induced knock-out of oxygen, creating thereby oxygen vacancies. These oxygen vacancies agglomerate with each other increasing the defect size and τ_2. Increase in defect size causes a decrease in concentration of defects in Bi-2212 with increasing dose, as evident from Table-II. In Bi-2223, the knock-out of oxygen is absent and hence there is no change in size of defects. Because of increase in size, there is a reduction in concentration of defects in Bi-2212 up to the dose of $5x10^{15}$ protons/cm^2 as seen from Table-II.

Irradiation dose (Protons/cm^2)	N (number of vacancies per vacancy cluster)	C (ppm)
Bi-2212		
Unirradiated	2	2.63
1x10^{15}	2	2.57
2x10^{15}	2	1.76
5x10^{15}	3	1.06
8x10^{15}	1	4.26
1x10^{16}	1	6.37
Bi-2223		
Unirradiated	1	5.10
1x10^{15}	1	5.25
2x10^{15}	1	5.25
5x10^{15}	1	5.30
8x10^{15}	1	5.45
1x10^{16}	1	5.55

Table II. Defect Size (N) and Concentration (C) in Bi-2212 and Bi-2223 as a function of dose.

Increase in defect size causes a decrease in concentration of defects in Bi-2212 with increasing dose, as evident from Table-II. At high dose of irradiation however, there will be appreciable generation of cationic vacancies too by displacement of either of Bi, Sr, Ca, Cu. There is a possibility of combination of a fraction of these cationic atoms with oxygen vacancies. This process can reduce the size of oxygen vacancies, which is reflected at a dose higher than 5x10^{15} protons/cm^2. In Bi-2223, the knock-out of oxygen is absent and hence there is no change in size of defects.

In the mixed state of a Type II superconductor with transport current, Lorentz force is exerted on magnetic flux lines which causes flux motion and energy dissipation. There are two categories of flux motion- flux flow and flux creep. In the former case, Lorentz force dominates and drives the flux lines. In the latter case, the flux pinning is strong and the flux lines move only by thermally activated jump from one pinning site to another. Magnetoresistance under high field in the superconducting state is a manifestation of this dissipation. Thus, the systematic study of the influence of an external magnetic field on resistive transition is an important source of information for Jc and pinning potential. So, DC electrical resistivity of irradiated as well as unirradiated BSCCO samples were measured in magnetic field.

The conventional Lorentz force induced dissipation plays a minor role in the high temperature part of resistive transition (i.e. near Tc(onset)) due to fluctuation of the superconducting order parameter which is very dominant in case of HTSC materials [30]. Only, in case of low temperature part of the resistive transition temperature (i.e. near Tc(R=0), dissipation energy due to motion of vortices by thermally activated flux creep plays an important role in pinning [31,32]. Hence, thermally activated flux creep model [48] was used to analyse the magnetoresistance of irradiated and unirradiated BSCCO samples in the temperature regime Tc(onset) to Tc(R=0). According to this model, the resistivity in this temperature regime is given as:

$$\rho(T,H) = \rho_0 \exp [-U(T,H)/(K_B T)] \quad (3)$$

where prefactor ρ_0 is a coefficient related to the vortex volume, the average hopping distance of vortices and the characteristic frequency with which vortices try to escape the potential well. Usually, ρ_0 is of the order of normal state resistivity near Tc(onset) [33]. ρ_0 in our case has been taken as the normal state resistivity at 100K and 125K for Bi-2212 and Bi-2223 respectively. The activation energy U(T,H) for various fields H has been extracted by using Arrhenius type equation (3) in the form:
$U(T,H) = (K_BT)\ln[\rho_0 / \rho(T,H)]$ based on $\rho(T)/\rho_0$. Finally, U(0,H) was determined from the plots of U(T,H) versus temperature fitted with the equation:

$$U(T,H) = U(0,H)\,[1-T/Tc(H)]^n \quad (4)$$

We have done the analysis in low temperature regime corresponding to flux creep, i.e. where $U(T,H) >> K_BT$ [34]. The best fit was obtained for n=2.
In Bi-2212, the pinning potential U(0,H) has increased with dose up to $5x10^{15}$ protons/cm^2. This is in tune with the increase in positron lifetime τ_2 in PAL studies and hence the increase in defect size from divacancy to trivacancy and thereby defects acting as more effective pinning centre. Beyond this dose, U(0,H) values have decreased with reduction in vacancy size from trivacancy to monovacancy. In Bi-2223, U(0,H) does not show any significant change with the dose of irradiation as seen in PAL studies. U(0,H) of unirradiated Bi-2223 is significantly higher than Bi-2212. The defect concentration of unirradiated Bi-2223 was also higher than Bi-2212 as revealed from Table-II.
Jc of proton irradiated as well as unirradiated BSCCO samples were evaluated from DC magnetisation studies at fields up to 1 Tesla. At the field higher than Hc_1, magnetic flux enters into the grain and hence the intragranular critical current density Jc can be evaluated using Clem-Bean formula [36,37]:

$$Jc = [30\Delta M] / a$$

where M is the magnetisation and 'a' is the average grain size of the samples taking into account the granularity in polycrystalline samples.
Jc versus H shows a clear exponential relation as:

$$Jc = Jc_0 \exp(-H/H_0),$$

where Jc_0 and H_0 are fitting parameters [38].
Jc_0 is defined as the critical current density at zero magnetic field. In Bi-2212, Jc and Jc_0 increase with dose up to $5x10^{15}$ protons/cm^2 and then decreases. But, in Bi-2223, there is no significant change up to this dose, though in the unirradiated stage, Jc and Jc_0 are higher for Bi-2223 owing to high defect concentration in the unirradiated stage, as discussed earlier.
At doses higher than $5x10^{15}$ protons/cm^2, there is a possibility of occupancy of cationic atom at the site of oxygen vacancies causing a decrease in defect size in Bi-2212. The smaller defects are less effective in pinning causing a reduction in pinning potential and Jc. On the other hand, in Bi-2223, there is a reduction in positron lifetime τ_2 implying the formation of vacancy loops acting as a weak trapping centre. This defect configuration might be deleterious in pinning, whereby there is a drastic fall in Jc in Bi-2223 above the dose of $5x10^{15}$ protons/cm^2.
Thus, there is one to one correspondence between defect size, pinning potential and Jc in Bi-2212 and Bi-2223. Moreover, difference in these two systems with respect to abovementioned properties is due to the difference with respect to the irradiation induced knock-out of oxygen.

5. Particle irradiation on MgB_2

In MgB_2, the irradiation studies with heavy ions on thin films [39] and protons on bulk materials [40] have not reflected any significant changes in T_c and other superconducting properties. Hence we employed heavy ions like Neon with large deposition energy and high values of displacements per atom (dpa) to bring about changes in bulk samples. There has not been significant change in Tc up to the dose of $1x10^{15}$Neon/cm^2. The plots of resistivity versus temperature for all the four samples are shown in Fig. 4. We observe that there is no significant change in Tc indicative of rather insensitivity of MgB_2 towards particle irradiation. There is slight decrease in Tc for the sample with the highest dose. The values of Tc and room temperature resistivity (ρ_{300}) are listed in Table III. There is almost no increase in ΔTc excepting at the highest dose. ρ_{300} of the polycrystalline samples increased with dose except for the lowest dose. The decrease in resistivity for the sample irradiated with the dose of $1x10^{13}$ Neon/cm^2 may be due to thermal annealing of the defects, which were initially present in the sintered sample leading to a decrease in the residual resistivity. At low dose of irradiation, mobile defects are also seen to increase the long-range ordering in partly ordered metallic alloys [41]. The depth of 160 MeV Neon ion implantation is 106μ, as obtained from Monte Carlo simulation using the code TRIM [6]. Displacement energy of both Mg and B has been 25eV with lattice binding energy of 3eV. The high binding energy of B is an outcome of strong sp^2 hybrid σ bonding between in-plane B atoms. The number of displacements/ion is 2734 as obtained from TRIM simulations. The dpa in the range of 106μ obtained thereby is $8.2x10^{-18}$/ion/cm^2. Energy loss here is larger by a factor of 10^2 than that caused by 6 MeV protons in MgB_2. Defect concentration at the highest dose is around 0.1% in the range of the projectile with fairly bulk damage.

As already stated, in MgB_2, the grains are strongly coupled which are not disturbed even after irradiation, as noticed by inappreciable change in ΔTc in contrast to HTSC cuprates. MgB_2 is a strongly coupled phonon mediated superconductor. The decrease in resistivity is

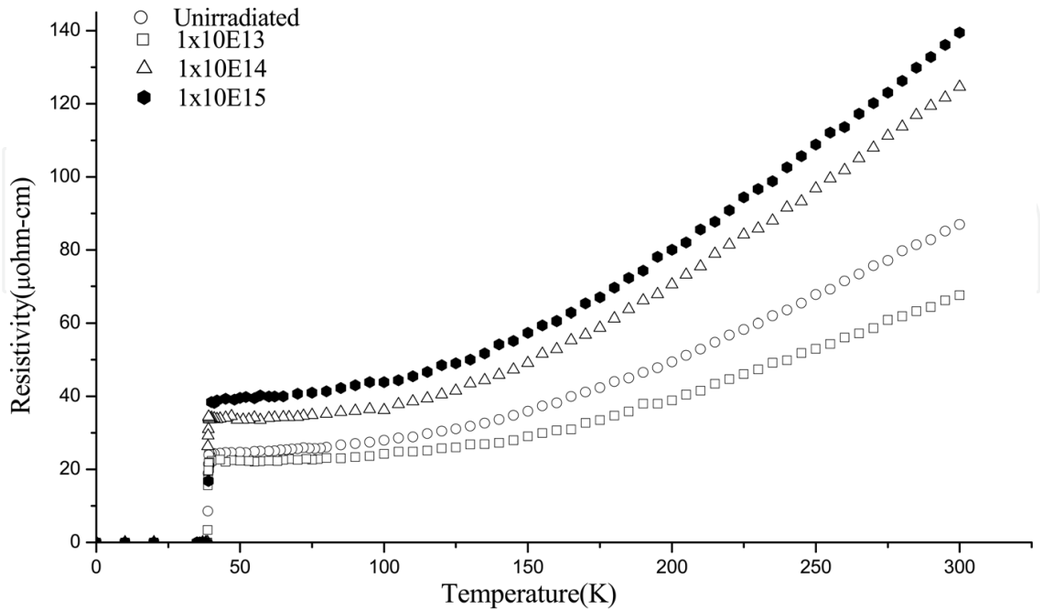

Fig. 4. Resistivity versus temperature. Though it is metallic, the resistivity is nonlinear.

Dose (ions/cm^2)	Tc (K)	ρ_0 (μΩ-cm)	ρ_{300} (μΩ-cm)	ρ' (μΩ-cm/K)	$\rho_{300} - \rho_0$ (μΩ-cm)
Zero	38.7	25.01	86.94	0.32	61.93
1X10^{13}	38.6	22.47	67.57	0.26	45.10
1X10^{14}	38.7	33.71	124.60	0.48	90.89
1X10^{15}	38.0	39.94	139.46	0.52	99.52

Table III.

linear with temperature from 300K up to a certain point (~ 200 K) and then it deviates from linearity. This shows that resistivity can be explained from phonon scattering mechanism. We have fitted the experimental curve to Bloch-Grüneisen expression [42],

$$\rho(T) = \rho_0 + (m-1)\rho'\Theta\left(\frac{T}{\Theta}\right)^m \int_0^{\frac{\Theta}{T}} \frac{x^m \exp(x)}{\left(\exp(x)-1\right)^2} dx \tag{5}$$

Here, ρ_0 is the residual resistivity, ρ' the temperature coefficient of resistivity and Θ the Debye temperature. ρ_0, ρ' and Θ are the fitting parameters. ρ(T) varies as T^5 at low temperature. The increase in resistivity has contributions from ρ_0 and ρ'. The increase of ρ_0 can be related to the increase in defect concentration and the damage at grain boundaries with irradiation. The decrease in ρ_0 at the lowest dose can be understood from annealing of the defects as already mentioned. Debye temperature did not vary much with irradiation and was from 903K to 909K (variation is within the error range of the fit).

We have obtained the EPC constant λ about 0.84 for the unirradiated sample using the experimentally obtained Tc and the fitted Θ value in the McMillan equation

$$T_c = \frac{\Theta}{1.45}\exp\left[\frac{-1.04(1+\lambda)}{\lambda-(1+0.62\lambda)\mu^*}\right] \tag{6}$$

with the value of Coulomb pseudopotential μ^* taken as 0.1 [43]. λ also has not changed significantly with irradiation due to insignificant variation of T_c and Θ.

The increase in ρ′ can be understood from bonding nature of MgB_2. As mentioned earlier, strong covalent σ-bonding within B-B layer gives rise to σ bands. The carriers of the σ bands are strongly coupled with the in-plane B E_{2g} stretching modes, giving rise to superconductivity [44,45]. Electron- phonon coupling constant along σ bands (λ_σ) governs Tc. The contribution to the conductivity is expected to be low in σ bands due to strong EPC. In two band system, the conductivity can be considered arising from the parallel network of the σ and π bands [43]. As compared to σ bands, conductivity would be large in π bands due to low EPC constant. The density of states around the Fermi surface ($N(E_F)$) of π band is 56% and that of σ bands is 44% [46]. So the normal state conductivity is mainly governed by the carriers of the metallic π bands.

Particle irradiation causes vacancies in both B and Mg layers. Irradiation induced B vacancies would damage both σ and π bonding network. π bonding network extends towards Mg ions as there is an interaction between them. Irradiation induced vacancies in both Mg and B sites affect the π bonding and hence $N(E_F)$ due to π-bonding. As ρ′ is inversely proportional to $N(E_F)$, decrease in $N(E_F)$ with irradiation causes an increase in ρ′.

There is no role of Mg ions with σ bonding hence no role in EPC and Tc. Irradiation induced B vacancies up to the dose of $1x10^{15}$ ions/cm^2 do not cause significant change in λ_σ and hence tc.

6. Upper critical field

Upper critical field $H_{c2}(T)$ was extracted from the magneto transport measurements from the intersection of the slopes at the points of resistivity at 40K (ρ_{40}) and at the point corresponding to $0.9\rho_{40}$. In Fig. 5, $H_{c2}(T)$ for samples A and B (A: Unirradiated & B: Irradiated) are plotted as a function of temperature. There has been only an appreciable increase in upper critical field with lowering of coherence length, which has got some significance in application.
$H_{c2}(0)$ was extracted using the formula:

$$H_{c2}(T) = H_{c2}(0)\left\{1-\left(\frac{T}{T_c}\right)^{\alpha}\right\}^{\beta} \tag{7}$$

with $\alpha = 2$ and $H_{c2}(0)$ and β as fitting parameter. β was found to be ~ 1.67 for unirradiated sample and 1.78 for irradiated sample. In MgB_2 single crystal $\mu_0 H_{c2}(0)$ is around 3.5T along *c* axis and around 15 to 17 T along *ab* direction [47, 48]. In polycrystalline sample where the grains are randomly oriented, $H_{c2}(0)$ is governed by the higher value of the $H_{c2}c$ and H_{c2}^{ab}. $\mu_0 H_{c2}(0)$ of the unirradiated sample is 18.7T and for the irradiated sample, it increases to 20.4T due to disorder introduced by Ne ion irradiation. There is a positive curvature of the H_{c2}–T near T_c. In MgB_2 single crystal this positive curvature is observed in $H_{c2}^{ab}(T)$ [47]. The positive curvature is believed to be characteristic of layered superconductors [49]. It seems that both the two-gap and the anisotropic gap model [50] can qualitatively explain the positive curvature of MgB_2 near T_c. But this feature is also observed in single gap superconductor or in isotropic (K,Ba)BiO_3 systems [51]. The curvature of the irradiated sample is greater than the unirradiated sample.
Using Ginzburg-Landau (GL) expression for B_{c2}:

$$\mu_0 H_{c2} = \left[\frac{\phi_0}{\left(2\pi\xi^2\right)}\right] \tag{8}$$

where, ϕ_0 is the quanta of flux *h/2e*, we obtain ξ(0) = 4.2 nm for the unirradiated sample A and 3.9 nm for B-slight reduction due to irradiation.

7. Critical current density

The magnetisation critical current density (J_c) was extracted using Bean's critical state model. J_c of the unirradiated sample A at 15K and 1.0T is around 10^5 Amp/cm^2. The value is quite high as compared to HTS like bismuth cuprate superconductor. However, there is a sharp fall of J_c with increasing B for the unirradiated sample like HTS. In case of the irradiated sample B, the magnetisation measurement shows J_c to be lower than the unirradiated sample A at low field but higher than A at high field as evident from Fig. 6.

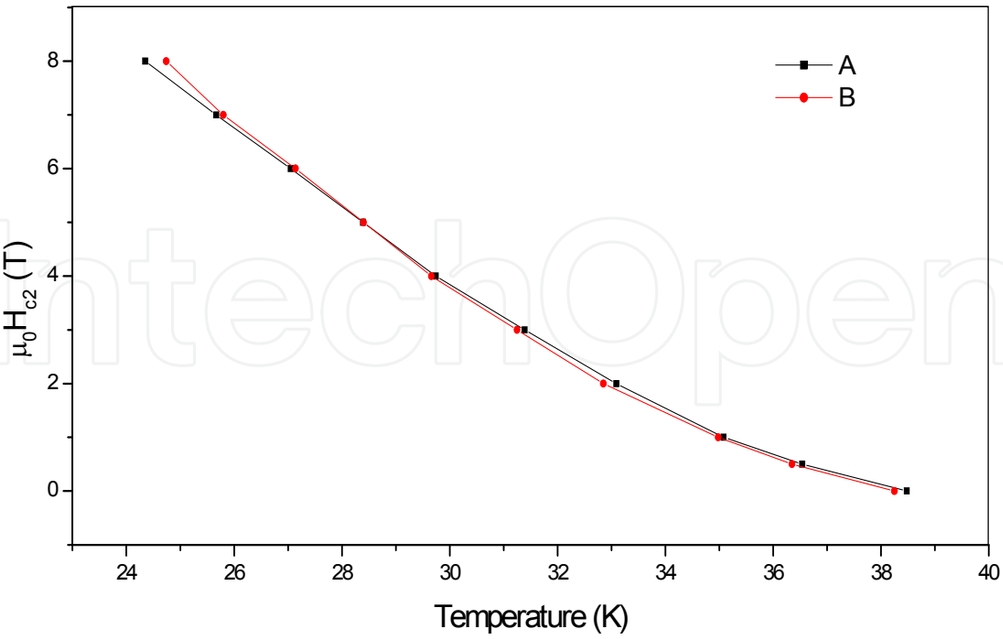

Fig. 5. Temperature variation of upper critical field for A & B.

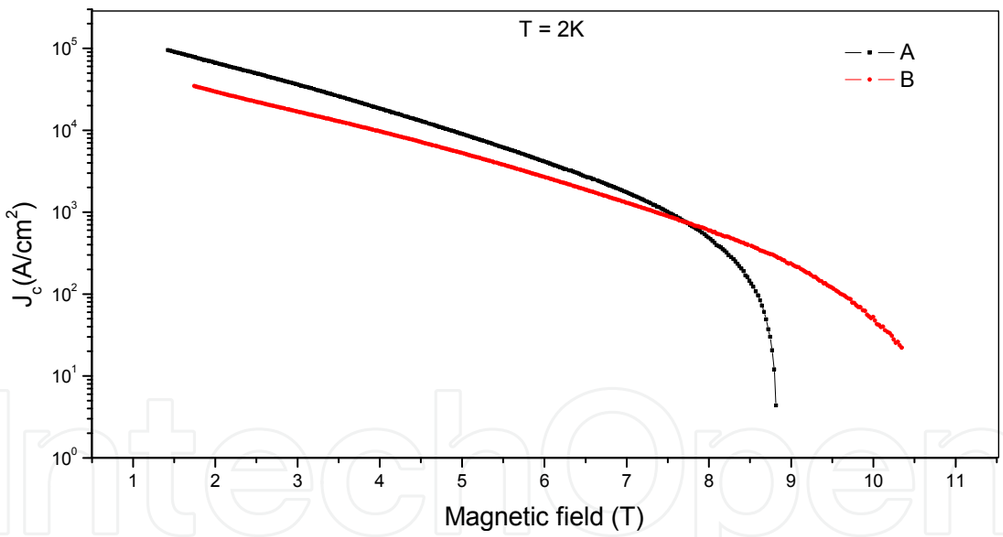

Fig. 6. Jc as a function of field. Jc for B is lower at low field but higher at high field .

$J_c(B)$ is governed by the nature of pinning and pinning force density. In order to see the effect of irradiation on pinning force density F_p ($F_p = J_c x H$), we have plotted $F_p(H,T)$ versus H in reduced scale. It is known that such curves form universal scaling at different temperatures [52]. In fig. 7, we have plotted fp ($f_p = F_p/F_p^{max}$) versus h ($h = H/H_{irr}$); F_p^{max} is the maximum value of F_p and H_{irr} is the irreversibility field at that particular temperature being explained as follows. In high temperature superconductors there exist a large region below the thermodynamic upper critical field (H_{c2}) line in H-T phase diagram (high T high H region) where the motion of the flux lines is reversible [53]. The lower boundary of this region is marked by a line called irreversibility line (IL). This region occurs in H-T phase

diagram due to some dissipative effects. In low temperature superconductors there is little or insignificant difference between IL and H_{c2} line. However, in HTS, IL is found to lie much below H_{c2} line. IL is attributed to a line above which the temperature enhances the classical Kim-Anderson flux creep or phase transition of flux line (like vortex-glass to liquid phase transition, melting of flux line lattice etc) [54, 55]. HTS has high critical temperature and at the same time they are highly anisotropic. Hence there is a large gap between IL and H_{c2} in HTS.
We have demonstrated a representative plot of fp versus h at 20 K (figure 7). There is a slight change between irradiated and unirradiated sample. We have fitted the curve using the generalized function:

$$f = ah^k (1-h)^m \tag{9}$$

The exponents k and m are 0.89 and 3.14 respectively for sample A and 0.61 and 2.22 respectively for sample B. Fig. 8 shows the 3D plot of F_p^{max}-H-T relation for the sample A. This shows that the pinning mechanism is somewhat altered due to Neon ion irradiation. The lower value of pinning force density F_p^{max} for irradiated sample B causes J_c to be lower than that of A at low field. But the lower values of the exponents for B in equation (9) show that F_p is higher for sample B than that of A at high field and hence J_c. This indicates that F_p decreases with applied magnetic field more slowly in case of B implying lower slope of J_c-B curve for sample B. The lower values of the exponents k and m of the irradiated sample show that there is reduction of the distance of the pinning centers (though to a low extent).

8. Conclusion

High temperature Cuprate superconductors (HTSC) are nonstoichimetric based on defects and disorders, which play a great role as carrier concentration and hence control Tc, Jc, resistivity etc. Particle irradiation induced defects modulate the carrier density through change in oxygen stoichiometry. In particular, irradiation induced oxygen vacancies act as flux pinning centres causing enhancement in Jc, pinning potential. Other cationic defects and disorder manifest,

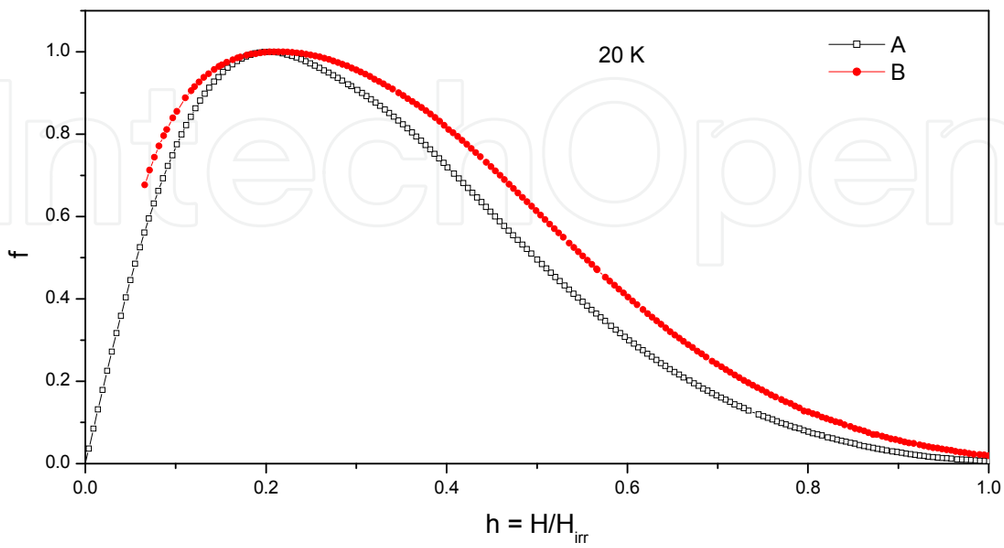

Fig. 7. Normalised pinning force versus magnetic field normalized with H_{irr}.

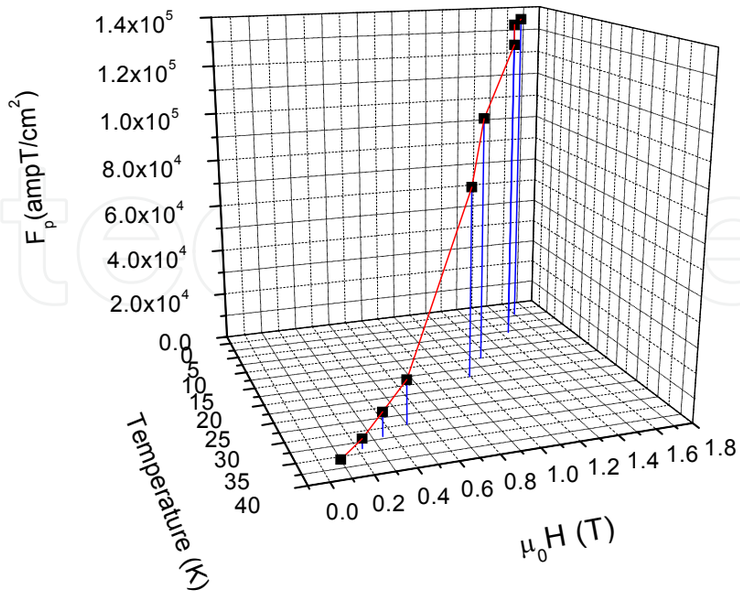

Fig. 8. 3D plot of pinning force density as function of temperature, magnetic field.

where this irradiation induced oxygen knock out is absent. We studied particle irradiation effects on Bi-based superconductors- Bi-2212 and (Bi,Pb)-2223. In Bi-2212 containing loosed excess oxygen needed for structural stability, particle irradiation causes knock-out of loose oxygen. In these systems, this excess oxygen plays the role of hole carrier. Hence, change of excess oxygen content due to particle irradiation causes a change in Tc (increase in the overdoped Bi-2212) and resistivity. Moreover, knocked out oxygen vacancies act as flux pinning centre for the enhancement of Jc. But, in Bi-2223, the presence of larger Pb(II) minimizes the presence of loose excess oxygen, and the irradiation induced oxygen knock-out is not the scenario. Hence there is no significant enhancement of Jc owing to irradiation. There is decrease in Tc and increase in resistivity. In both systems, there is a metal to insulator transition above the fluence of $1x10^{16}$α/cm^2, but, the reasons are different. Lowering of oxygen carrier concentration is the cause in Bi-2212 and in Bi-2223, localization due to irradiation induced disorder is the prime factor. Thus, HTSC's are in general very much sensitive to particle irradiation, whether by lowering of carrier concentration or, by generation of irradiation induced disorder. On the other hand, MgB_2, which is an intermediary between conventional superconductors and HTSC's is fairly insensitive to irradiation. It is a multiband BCS type phonon mediated superconductor. Strong covalent σ-bonding within B-B layer gives rise to σ bands and carriers of σ bands are strongly coupled with the in-plane B E_{2g} stretching modes, giving rise to superconductivity. Electron- phonon coupling constant along σ bands (λ_σ) governs Tc, which is not significantly affected by heavy ion like neon irradiation, even at the fluence of $1x10^{15}$ ions/cm^2. In two band system, the conductivity can be considered arising from the parallel network of the σ and π bands. As compared to σ bands, conductivity would be large in π bands due to low EPC constant. Particle irradiation affects the π band network. Hence, there is an appreciable increase in resistivity without any significant decrease in Tc and also, the role of irradiation induced defects in intragranular pinning is insignificant. The grain boundary pinning is the dominant scenario in case of MgB_2 as evident from magnetization and

magnetoresistance measurements. We also studied the enhancement of Jc by doping Mg with Hf (1%). The enhancement was enormous! The contribution was from other borides precipitating at the grain boundary.

9. References

[1] S.K.Bandyopadhyay, P.Barat, S.K.Kar, U. De, A.Poddar, P.Mandal, B.Ghosh, and C.K.Majumdar, Solid State Communications 82 (1992) 397.
[2] S.K.Bandyopadhyay, P.Barat, Pintu Sen, A.K.Ghosh, A.N.Basu and B.Ghosh, Phys. Rev. B58 (1998) 15135.
[3] G.Linker, J.Geerk, T.Kroener, O.Meyer, J.Remmel, R.Smithey, B.Strehlau, and X.X.Xi, Nucl. Inst. Meth. in Phys. Res.B59-60 (1991) 1458.
[4] O.Meyer, in Studies of High Temperature Superconductors, ed. A.V.Narlikar, V. 1. (Nova Science Publishers, New York, 1989); p. 139 and. the references therein.
[5] P. Sigmund, Radiation Effects 1 (1969) 15; M.J.Norgett, M.T.Robinson and I.M.Torrens, Nucl. Eng. De sign 33 (1974) 50.
[6] J.P.Biersack and L.G.haggmark, Nucl. Inst. & Meth. 174 (1980) 257.
[7] R.Viswanathan and R.Certon, Phys. Rev. B18 (19780 15.
[8] L.R.Testardi and L.F.Matthews, Phys. Rev. Lett. 41 (1978) 1612.
[9] B.D.Weaver, E.M.Jackson, G.P.Summers and E.A.Burke, Phys. Rev. B46 (1992) 1134; and references therein.
[10] G.P.Summers, D.B.Chrisley, W.G.Maisch, G.H.Strauss, E.A.Burke, M.Nastasl and J.R.Tesmer, IEEE Trans. On Nucl. Sci. 36 (1989) 1840.
[11] G.C.Xiong, H.C.Li, G.Linker and O.Meyer, Phys. Rev. B38 (1988) 1; Physica C153-155 (1988) 1447.
[12] G.J.Russell, H.B.Sun and K.N.R.Taylor, Physica C241 (1995) 219.
[13] C.Allgeier and J.S.Schilling, Physica C168 (1990) 499.
[14] J.M.Tarascon, Y.LePage, P.Bardoux, B.G.Bagley, L.H.Greene, W.R.McKinnon, G.W.Hull, M.Giroud and D.M.Hwang, Phys. Rev. B37 (1988) 9382.
[15] T.Tamegai, K.Koga, K.Suzuki, M.Ichimara, F.sakai and Y.Iye, Jpn. J. Appl.Phys. 28 (1989) L112.
[16] R.Yoshizaki, Y.Saito, Y.abe and H.Ikeda Physica C152 (1988) 408.
[17] J.B.Torrance, Y.Tokura, A.I.Nazzal, A.Bezinge, T.C.Huang and S.S.P.Parkin, Phys. Rev. Lett. 61 (1988) 1127.
[18] Y.Shimakawa, Y.Kubo, T.Manako and H.Igarashi, Phys. Rev. B40, (1989)11400.
[19] A.Matsuda, K.Kinoshita, T.Ishii, H.Shibata, T.Watanabe and T.Yamada, Phys. Rev. B38 (1988) 2910.
[20] Z.Z.Wang, J.Clayhold, N.P.Ong, J.M.Tarascon, L.H.Greene, W.R.McKinnon and G.W.Hull, Phys. Rev. B36 (1987) 7222.
[21] P.Mandal, A.Poddar, B.Ghosh and P.Choudhury, Phys. Rev B43 (1991)13102 .
[22] P.W.Anderson, Phys. Rev. 109 (1958) 1492.
[23] R.A.Fisher, S.Kim, S.E.Lacy, N.E.Phillips, D.E.Morris, A.G.Markelz, J.Y.T.Wei and D.S.Ginley, Phys. Rev. B 38 (1988) 11942.
[24] N.Okazaki, T.Hasegawa, K.Kishio, K.Kitazawa, A.Kishi, Y.Ikeda, M.Takano, K.Oda, H.Kitaguchi, J.Takada and Y.Miura, Phys. Rev.B 41 (1990) 4296.
[25] H.Zhang and H.Sato, Physica C214 (1993) 265.
[26] F.S.Galasso, Structure, Properties and Preparation of Perovskite-Type Compounds (Pergamon. , New York, 1969) p. 4

[27] S.B.Samanta, P.K.Dutta, V.P.S.Awana, E.Gmelin and A.V.Narlikar, Physica C178 (1991) 171.
[28] S.K.Bandyopadhyay, Pintu Sen, P.Barat, P.Mukherjee, S.K.Das and B.Ghosh, Pramana, Journal of Physics 47, 309 (1996); S.K.Bandyopadhyay, A.K.Ghosh, P.Barat, Pintu Sen, A.N.Basu and B.Ghosh, Phys. Stat. Sol. A162 (1997) 701.
[29] M.J.Puska and R.M.Nieminen, J.Phys. F : Metal Phys 13 (1983) 333.
[30] D.H.Kim, D.J.Miller, J.C.Smith, R.A.Holoboff, J.H.Kang and J.Talvacchio, Phys. Rev. B44 (1991) 7607.
[31] R.Ikeda, T.Ohmi and T.Tsuneto, Phys. Rev. Lett. 67 (1991) 3874.
[32] O.Brunner, L.Antognazza, J.M.Triscone, L.Miévelle and Ø.Fisher, Phys. Rev. Lett. 67 (1991) 1354.
[33] T.T.M.Palstra, B.Batlogg, R.B.van Dover, L.F.Schneemeyer and J.V.Waszczac, Phys. Rev. B41 (1990) 6621.
[34] C.Attanasio, C.Coccorese, V.N.Kushnir, L.Maritato, S.L.Prischepa and M.Salvato, Physica C255 (1995) 239.
[35] M.D.Lan, J.Z.Liu, Y.X.Jia, L.Zhang, Y.Nagata, P.Klavins and R.N.Shelton, Physica C218 (1993) 69.
[36] Shin-Pei Matsuda, T.Doi, A.Soeta, T.Yuasa, N.Inoue, K.Aihara and T.kamo, Physica C185-189 (1991) 2281.
[37] W.M.Chen, S.S.Jiang, Y.C.Guo, J.R.Jin, X.S.Wu, X.H.Wang, X.Jin, X.N.Xu, X.X.Yao and S.X.Dou, Physica C 299 (1998) 77.
[38] J.Fontcuberta, S.Pinol, X.Obradors, F.Lera and C.Rillo, Cryogenics 30 (1990) 656.
[39] A Gupta, H. Narayan, D. Astil, D. Kanjilal, C. Ferdeghini, M. Paranthaman and A.V. Narlikar, Supercond. Sci. Technol. 16 (2003) 951-955.
[40] E. Mezzeti, D. Botta, R. Cherubini, A. Chiodoni, R. Gerbaldo, G. Ghigo, G. Giunchi, L. Gozzeline and B. Minetti, Physica C 372-376 (2002) 1277.
[41] E.M. Schulson, J Nucl. Mater. 83 (1979) 239.
[42] Y. Kong, O.V. Dolgov, O. Jepsen and O.K. Anderson, Phys. Rev. B 64 (2001) 020501(R).
[43] I.I. Mazin and V.P. Antropov, Physica C 385 (2003) 49.
[44] A.Y. Liu, I.I. Mazin and J. Kortus, Phys. Rev. Lett. 87 (2001) 087005.
[45] J.Kortus, I.I. Mazin, K.D. Belashchenko, V.P. Antropov and L.L.Boyer, Phys. Rev. Lett. 86 (2001) 4656.
[46] H.J. Choi, M.L. Cohen and S.G. Louie, Physica C 385 (2003) 66.
[47] M. Zehetmayer, M. Eisterer, J. Jun, S.M. Kazakov, J. Karpinski, A. Wisniewski, and H. W. Weber, Phys. Rev. B 66 (2002) 052505.
[48] L. Lyard, P. Samuely, P. Szabo, T. Klein, C. Marcenat, L. Paulius, K.H.P. Kim, C.U. Jung, H.S. Lee, B. Kang, S. Choi, S.I. Lee, J. Marcus, S. Blanchard, A.G.M. Jansen, U. Welp, G. Karapetrov and W. K. Kwok, Phys. Rev. B 66 (2002) 180502.
[49] J.A. Woollam, R. Somoano and P.O'Connor, Phys. Rev. Lett. 32 (1974) 712.
[50] A.I. Posazhennikova, T. Dahm and K. Maki, Europhys. Lett., 60 (2002) 134.
[51] S. Blanchard, T. Klein, J. Marcus, I. Joumard, A. Sulpice, P. Szabo, P. Samuely, A. G. M. Jansen, and C. Marcenat, Phys. Rev. Lett. 88 (2002) 177201.
[52] D. Dew-Hughes, Phil. Mag. 55, (1987) 459.
[53] Y. Yeshurun and A.P. Malozemoff, Phys. Rev. Lett. 60 (1988) 2202.
[54] M.P.A. Fisher, Phys. Rev. Lett. 62 (1989) 1416.
[55] A. Houghton, R.A. Pelcovits and S. SudbØ, Phys. Rev. B, 40 (1989) 6763.

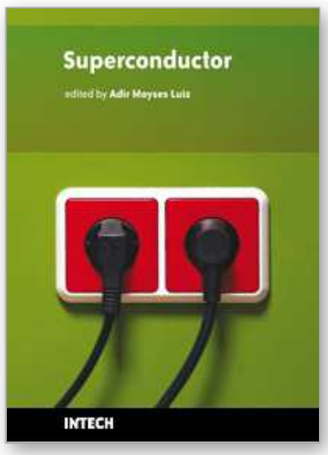

Superconductor
Edited by Doctor Adir Moyses Luiz

ISBN 978-953-307-107-7
Hard cover, 344 pages
Publisher Sciyo
Published online 18, August, 2010
Published in print edition August, 2010

This book contains a collection of works intended to study theoretical and experimental aspects of superconductivity. Here you will find interesting reports on low-Tc superconductors (materials with Tc< 30 K), as well as a great number of researches on high-Tc superconductors (materials with Tc> 30 K). Certainly this book will be useful to encourage further experimental and theoretical researches in superconducting materials.

How to reference
In order to correctly reference this scholarly work, feel free to copy and paste the following:

Sujit Kumar Bandyopadhyay (2010). Charged Particle Irradiation Studies on Bismuth Based High Temperature Superconductors and MgB2: a comparative study, Superconductor, Doctor Adir Moyses Luiz (Ed.), ISBN: 978-953-307-107-7, InTech, Available from: http://www.intechopen.com/books/superconductor/charged-particle-irradiation-studies-on-bismuth-based-high-temperature-superconductors-and-mgb2-a-co

INTECH
open science | open minds

InTech Europe
University Campus STeP Ri
Slavka Krautzeka 83/A
51000 Rijeka, Croatia
Phone: +385 (51) 770 447
Fax: +385 (51) 686 166
www.intechopen.com

InTech China
Unit 405, Office Block, Hotel Equatorial Shanghai
No.65, Yan An Road (West), Shanghai, 200040, China
中国上海市延安西路65号上海国际贵都大饭店办公楼405单元
Phone: +86-21-62489820
Fax: +86-21-62489821

IntechOpen